Erratum

Polycomb group protein complexes exchange rapidly in living *Drosophila*

Gabriella Ficz, Rainer Heintzmann and Donna J. Arndt-Jovin *Development* **132**, 3963-3976.

The e-press version of this article that was published on the 3rd August contains an error in Equation 1 and the preceding sentence on p. 3965.

Both the published print and online versions of this article are correct.

We apologise to the authors and readers for this mistake.

Polycomb group protein complexes exchange rapidly in living *Drosophila*

Gabriella Ficz[1], Rainer Heintzmann[1,2] and Donna J. Arndt-Jovin[1,*]

[1]Max Planck Institute for Biophysical Chemistry, Department of Molecular Biology, 37070 Göttingen, Germany
[2]King's College London, Randall Division of Cell and Molecular Biophysics, New Hunt's House Guy's Campus, London SE1 1UL, UK
*Author for correspondence (e-mail: djovin@gwdg.de)

Accepted 21 June 2005

Development 132, 3963-3976
Published by The Company of Biologists 2005
doi:10.1242/dev.01950

Summary

Fluorescence recovery after photobleaching (FRAP) microscopy was used to determine the kinetic properties of Polycomb group (PcG) proteins in whole living *Drosophila* organisms (embryos) and tissues (wing imaginal discs and salivary glands).

PcG genes are essential genes in higher eukaryotes responsible for the maintenance of the spatially distinct repression of developmentally important regulators such as the homeotic genes. Their absence, as well as overexpression, causes transformations in the axial organization of the body. Although protein complexes have been isolated in vitro, little is known about their stability or exact mechanism of repression in vivo.

We determined the translational diffusion constants of PcG proteins, dissociation constants and residence times for complexes in vivo at different developmental stages. In polytene nuclei, the rate constants suggest heterogeneity of the complexes. Computer simulations with new models for spatially distributed protein complexes were performed in systems showing both diffusion and binding equilibria, and the results compared with our experimental data. We were able to determine forward and reverse rate constants for complex formation. Complexes exchanged within a period of 1-10 minutes, more than an order of magnitude faster than the cell cycle time, ruling out models of repression in which access of transcription activators to the chromatin is limited and demonstrating that long-term repression primarily reflects mass-action chemical equilibria.

Key words: Polycomb group proteins, FRAP, Inverse FRAP, iFRAP, Transcription, Repression, Homeotic genes

Introduction

The activity of genes in eukaryotic organisms is modulated by non-histone chromatin-binding proteins. Both global and local chromatin states are transmitted from one cell generation to another (Grewal and Moazed, 2003; Phair et al., 2004; Vermaak et al., 2003). However, data are lacking on the lifetime of chromatin-bound protein complexes, such that the actual mechanisms by which they exert their activation or repression are not understood. Early in *Drosophila* development, a particular expression pattern of homeobox-containing (HOX) genes is established along the anteroposterior axis of the organism (Lewis, 1978) by transcriptional activators and repressors whose presence is only temporary and encoded by gap and pair-rule genes (Gaul and Jäckle, 1989; Tautz, 1988), whereas maintenance of the expression pattern is obligatory throughout development. Disturbance of the pattern leads to a switch of the determined state and homeotic transformations of the organism (Bienz and Muller, 1995; Busturia and Morata, 1988; Garcia-Bellido et al., 1976; Lewis, 1963).

The Polycomb group (PcG) and Trithorax group (trxG) of proteins are chromatin-binding proteins responsible for conserving the transcriptional state of the HOX genes and thereby cell identity. PcG proteins are responsible for the persistence of silencing whereas the trxG proteins are required for transcription in the active domains (Francis and Kingston, 2001; Levine et al., 2004; Orlando, 2003). PcG proteins are targeted to particular regions of the genome called Polycomb response elements (PREs) (Chan et al., 1994; Orlando et al., 1998; Strutt et al., 1997) where they act in multicomponent complexes to repress transcription of their target genes. The continued presence of PcG proteins on the PREs throughout development is required for silencing since deletion of the PRE (Busturia et al., 1997) or individual PcG genes (Beuchle et al., 2001) anytime during development of the organism results in gene derepression. Interestingly, although PcG complexes maintain the repression pattern for up to 10 cell generations most of the PcG protein complement dissociates at every mitosis (Buchenau et al., 1998).

There exist experimental data for the association of the PcG proteins with specific chromatin sequences, including the first observations by immunofluorescence on polytene chromosomes (Chiang et al., 1995; Franke et al., 1992; Rastelli et al., 1993). In vivo crosslinking and chromatin immunoprecipitation (ChIP analysis) of PcG proteins have preferentially detected high levels of proteins of the PCC (Polycomb core complex), and recently, also of Pleiohomeotic (Pho) and Enhancer of zeste [E(Z)], on PREs and promoters of known homeobox genes (Breiling et al., 2004; Ringrose et al., 2003; Strutt and Paro, 1997; Wang et al., 2004). Several models

have been proposed for the mechanism of PcG-mediated repression, such as (1) heterochromatinization or formation of a closed chromatin conformation that does not allow access to promoters; (2) inhibition of the assembly of the preinitiation transcription complex; and (3) interference with transcription initiation and/or elongation (Min et al., 2003; Paro and Hogness, 1991; Simon and Tamkun, 2002). Experimental evidence can be found to support each of the models. For example, PcG complexes reduced accessibility for large RNA polymerases over large stretches of DNA in the bithorax homeobox gene cluster (BX-C) (Fitzgerald and Bender, 2001), thereby inhibiting transcription of reporter genes, although restriction enzymes retained DNA access. However, the presence of PcG proteins at the *Ubx* promoter in wing imaginal discs (Wang et al., 2004) lends support to a direct inhibition of transcription, although perhaps only at the elongation rather than at the initiation step as has been suggested for the heat shock protein 26 (hsp26) promoter (Dellino et al., 2004).

Two different multiprotein polycomb repression complexes (PRCs) have been isolated and characterized biochemically. PRC2 (Ng et al., 2000) is composed of the PcG proteins, Extra sex combs (Esc), Suppressor (12) of zeste [Su(z)12] and histone-binding Nurf-55 and Enhancer of zeste [E(Z)], the latter of which methylates histone H3 at lysine 27 both in vivo and in vitro (Cao et al., 2002; Czermin et al., 2002; Kuzmichev et al., 2002; Müller et al., 2002; Yamamoto et al., 2004), thus marking nucleosomes for assembly of repression complexes. PRC1, which contains equimolar quantities of Polycomb (Pc), Polyhomeotic (Ph), Posterior sex combs (Psc) and Sex combs extra (Sce/dRing1), all of which have been shown to be essential for PcG silencing. Other PcG and non-PcG proteins such as Sex combs on midleg (Scm), heat-shock protein cognate 4 (Hsc4) and Zeste (Z), and some transcription factors have been isolated with PRC1 in non-stoichiometric amounts, implying the presence of more than one type of polycomb repression complex (Levine et al., 2002; Mulholland et al., 2003; Saurin et al., 2001).

Whether the in vitro isolated or assembled complexes represent truly competent repression machineries is a matter of debate, as will be discussed later. In vivo data imply that functional complexes are assembled sequentially, directly and with a particular hierarchy, on the chromatin itself (Buchenau et al., 1998; Wang et al., 2004) and single PcG gene deficiencies such as *E(Z)* result in loss of complex formation on PREs, although all of the proteins involved in the PCC or PRC1 are still present (Rastelli et al., 1993; Wang et al., 2004). For a complete understanding of the repression mechanism, we need to know the stability and lifetime of functional repression complexes in the living organism. Recently, it was reported that Polycomb can be competed away from genomic sites by methylated histone tail peptides in permeabilized salivary gland nuclei (Ringrose et al., 2004). However, no data have been available about binding equilibria and dissociation rate constants of any multiprotein PcG chromatin complex in vivo. In this study, we addressed this problem by performing photobleaching experiments (fluorescence recovery after photobleaching, FRAP) on GFP fusion proteins of Polycomb (Pc) and Polyhomeotic (Ph), two essential members of the PCC in whole living *Drosophila* embryos and larval tissues to determine their diffusion, binding equilibria and residence times. We measured these values in living organisms at different stages of development to determine whether there are changes in the stability of the complexes. By taking advantage of the polytene nature of the salivary gland chromosomes, we assessed the uniformity of the complexes between individual bands. The actual forward and reverse rate constants for complex formation were determined. Most of the complexes exchange within a period of 1 minute and all of the complexes in less than 10 minutes. We discuss the compatibility of these data with present models for repression and draw inferences about the homogeneity of the repression complex.

Materials and methods

Construction of *PhGFP*

The *Ph* (*proximal*) gene was fused to green fluorescent protein (*PhGFP*) using the strategy described in Netter et al. (Netter et al., 2001). It was cloned with both a *UAS* and a *Pc* promoter to provide controlled expression at different stages of fly development. The predicted *Pc* promoter (Neural Network Promoter prediction program of the Berkeley *Drosophila* Genome Project) was isolated from a *Pst*I fragment of the *Pc* genomic clone (kind gift of Jürg Müller) (Paro and Hogness, 1991) by amplification of a 559 bp fragment using the primers (5′-TTTAGATCTCAATTTGTGATACAATAAGTG-3′ and 5′-CCCGAGCTCATCTTAGCAAGTAGCCGTGTC-3′) and inserted as an *Eco*RI fragment upstream of the *Ph* protein-coding sequence (kind gift from Jürg Müller). The resulted fusion was inserted as a *Bgl*II-*Not*I fragment into the *pUAST* vector (Brand and Perrimon, 1993). Transgenic lines containing the construct *P[UAS,Pc:PhGFP]* were generated with standard transformation protocols using the w^{1118} host line (Spradling and Rubin, 1982) and the site of chromosome integration was determined genetically. The *Pc* promoter alone drives expression of PhGFP in the salivary gland nuclei. Expression of PhGFP in embryos and larval wing imaginal discs was induced with the Gal4 drivers listed below.

Fly strains and culture

The following strains were used in this study:

w^{1118}*; P{pPc-PcGFP,*w^{+}*}*;

w^{1118}*; P{UAS,Pc-PhGFP,* w^{+}*}*;

yw; P{en2.4-GAL4}e22c/SM5 (to drive expression of *phGFP* in embryos);

P{Gal4;w^{+}*}*Bx^{MS1096} (to drive expression of *phGFP* in wing imaginal discs) where it drives the expression of Gal4 in the whole wing blade (Capdevila and Guerrero, 1994).

All strains were maintained on standard corn-agar medium at 18°C and experiments were carried out at 25°C. The *PcGFP* stock was kindly provided by R. Paro (Dietzel et al., 1999) and the *en:Gal4* and Bx^{MS1096}*:Gal4* (Milan et al., 1998) drivers were provided by H. Jäckle.

Mounting of specimens for microscopy and imaging

For live imaging dechorionated embryos were transferred to a chamber with a coverslip bottom (LabTek) in oxygenated Tyrode's buffer (135 mM NaCl, 10 mM KCl, 0.4 mM $MgCl_2$, 1 mM $CaCl_2$, 5.6 mM glucose, 10 mM HEPES, pH 7.2). In order to prevent movement and buffer evaporation, they were covered with a polycarbonate membrane with 8 μm pores that allowed oxygen exchange (Nucleopore). Larval imaginal and salivary gland tissues were dissected in PBS and immediately transferred to similar chambers and covered with a Whatman 3M filter paper soaked in Tyrode's buffer. Imaging was performed at 21°C for a maximum of 2 hours after mounting with a 63× N.A. 1.2 water immersion objective using an inverted Zeiss LSM 510META microscope. GFP was excited with the 488 nm line of an Ar ion laser and emission collected between 505 and 545 nm with a pinhole equivalent to 2 Airy discs.

Photobleaching methods and image processing

FRAP images in somatic cell nuclei were performed with an XY sampling of 0.10 μm/pixel and in polyploid salivary gland nuclei, at 0.14 μm/pixel. Photobleaching was carried out for ~200 ms (FRAP in salivary gland nuclei) at ~200 μW laser power (measured through the objective). Pre-bleach and post-bleach images were acquired at high scanning speed with minimal laser intensity (AOTF 2%, ~5 μW). At later measurement times (after frame 20), the interval between scans was increased in order to reduce bleaching during monitoring.

3D-iFRAP

Three dimensional inverse FRAP (3D-iFRAP) experiments in embryos and imaginal discs were carried out by bleaching the whole nucleus except for a small region surrounding a fluorescent locus of interest for ~4 seconds. A time series of seven confocal z sections (with 5 second intervals between stacks for PhGFP and 10 seconds for PcGFP) were recorded for ~120 seconds after bleaching. The time stacks were aligned using a 3D tracking algorithm (View5D information can be found at http://wwwuser.gwdg.de/~rheintz/View5D/) developed in this laboratory. After alignment, the spot intensity was calculated using a weighted region of interest.

Image processing and fitting algorithms

Background fluorescence in all photobleaching experiments was measured in a user-defined field outside the tissue for each experiment separately or estimated directly from the acquired image. An average loss of fluorescence intensity during imaging was corrected for in the evaluation of FRAP and iFRAP data via normalization to time-dependent average intensity plots from separate nuclei imaged under identical conditions to the FRAP and iFRAP experiments. This correction was always less than 10%. The relative increase (FRAP) or decrease (iFRAP) in fluorescence intensity, corrected for background and bleaching during recovery, was normalized to the pre-bleach value and these $I_{norm,i}$ values were plotted for each time point:

$$I_{norm,i} = \frac{I_i - BG}{I_0 - BG} \cdot \frac{I_0^{ref} - BG}{I_i^{ref} - BG}\,, \tag{1}$$

where BG is the background intensity, I_i is the average intensity of the ROI in image i, I_0 is the pre-bleach intensity in the ROI, I_0^{ref} is the pre-bleach average intensity of an unbleached reference cell and is the intensity of the reference cell at image i. In the salivary gland nuclei, the total photobleaching during monitoring was less than 5%, obviating the need for a bleach correction during recovery. Images were corrected for XY drift by cross-correlation prior to quantification. In the 3D-iFRAP experiments, the spot intensity was calculated in three dimensions using a weighted region of interest after an alignment based on a tracking algorithm (using the View5D plugin to ImageJ developed in this laboratory). The half-maximum recovery time (t_0) in FRAP in preblastoderm embryos, the time required for the fluorescence intensity to recover halfway between the first post-bleach level and the final height of the recovery curve, was determined by fitting the recovery curves to the following function:

$$y = a + b \cdot \frac{t}{t + t_0}\,, \tag{2}$$

where t_0 corresponds to the half-maximum recovery time, a is the offset of the curve and b is the amplitude of the recovery curve. The diffusion constant was calculated using the translational diffusion equation described by Axelrod et al. (Axelrod et al., 1976):

$$D = \frac{w^2}{4 \cdot t_0} \cdot \gamma_D\,, \tag{3}$$

where w is the radius of the bleach spot (μm), t_0 is the half maximum recovery time (s) and γ_D is the correction factor for the shape of the bleaching beam. Using computer simulations, we calculated the correction factor, taking into account the diameter of the nucleus (8 μm for the preblastoderm nucleus and 25 μm for the salivary gland nucleus) with the half-width of the bleach box as w (0.75 μm for the preblastoderm nucleus and 1.75 μm for the salivary gland nucleus), which yielded a γ_D of 0.97 and 1.03 for the preblastoderm nuclei and salivary gland nuclei, respectively.

In FRAP experiments on bands of PcG proteins in salivary gland nuclei, the free signal was estimated by averaging the intensity in each frame near the spot in a region as defined by the lowest 30% voxels of the sum intensity projection over all aligned pre-bleach frames (see Fig. 7). This nucleoplasmic signal of the free protein estimated frame by frame was subtracted from each pixel and the total bound protein was determined as the sum of all pixels in the mask region of the 30% brightest pixels in the projection over all aligned pre-bleach frames.

Recovery curves were fitted with a single exponential function after excluding the first 30 seconds after bleaching, during which diffusion still influences the data in spite of the correction for free protein:

$$y = a + b \cdot (1 - e^{-t/t_0})\,, \tag{4}$$

where t_0 is the time required for the fluorescence intensity to reach ~63% of the final height of the recovery curve for the bound molecules, a is the offset of the curve and b is the amplitude of the recovery curve. According to our grid-based simulations, the influence of a spatially extended area of binding sites influences the binding kinetics in combination with the diffusion. The simulations also showed that there is only a minor influence of the size of a spot on its recovery kinetics as long as the total number of binding sites does not change. In other words, if an intense spot is doubled in size but has only half the concentration of binding sites, its recovery kinetics remain very similar. In addition, if the number of binding sites is doubled along with a doubling of the concentration of free molecules, the kinetics does not change. As the measured spots all have different sizes and intensities, we correct the measured single exponential recoveries according to our model. We define

$$B_{ratio} = \frac{I_{bound} - I_{nuc}}{I_{nuc}} \cdot P_{bound}\,, \tag{5}$$

where B_{ratio} is the ratio of total bound protein in the locus to the average free protein in a pixel, where I_{bound} is the mean intensity of the 30% highest pixels in the ROI, I_{nuc} is the mean intensity of the 30% lowest pixels in the ROI (free protein in the nucleoplasm) and P_{bound} is the number of pixels in the mask region of the bound molecules.

Simulations showed an approximately linear dependence of the t_0 values to the B_{ratio} of a locus using several fixed dissociation rate constants in the range previously found from iFRAP measurements in imaginal discs and a diffusion constant derived from the experimental data (D=0.5 μm^2 second^{-1}) as is shown by the lines in Fig. 8. The recovery times (t_0) for the measured data were corrected for this dependence according to the approximation (Eqn 6):

$$t_0^* = t_0 - \frac{B_{ratio}}{1.23\ \mu m^2}\,, \tag{6}$$

where t_0 is the experimental FRAP recovery time for individual loci as shown in Fig. 8B and 1.23 μm^2 is the slope of the simulation curves in Fig. 8B. The resulting dissociation rate constants for each individual locus are derived from the equality k_{off}=1/t_0*. These values are plotted in Fig. 9 against the B_{ratio} normalized by equating the highest ratio to 1, whereby there is no obvious correlation of the dissociation rate constants to the number of binding sites in a locus.

The pseudo reassociation rate constant k_{on}* was calculated

according to the method described by Sprague et al. (Sprague et al., 2004) that defines a pseudo-first-order rate constant given by

$$k_{on}^{*} = k_{off} \cdot \frac{C_{eq}}{F_{eq}} \quad (7)$$

$$k_{on} = \frac{k_{on}^{*}}{C_{s}}, \quad (8)$$

where k_{on}^{*} is the pseudo first order association rate constant, k_{on} is the second order association rate constant, C_s is the unknown concentration of binding sites, C_{eq} is the concentration of bound protein at equilibrium (mean intensity of the bound fraction) and F_{eq} is the concentration of the free protein at equilibrium (mean intensity in the nucleoplasm).

Western blots

Crude extracts were prepared from embryos of different developmental stages and larval tissues using lysis buffer [20 mM HEPES-KOH pH 7.5, 100 mM KCl, 2 mM EDTA, 0.5% Triton X-100, 0.3 U/ml aprotinin, 10 μg/ml leupeptin, 100 μg/ml soy bean trypsin inhibitor, protease inhibitor cocktail tablets (Roche Diagnostics), 5 mM DTT, 1 mM $MgAc_2$]. Proteins were separated on NuPage 4-12% Bis-Tris or NuPage 3-8% Tris-acetate polyacrylamide gels, and western blots were probed with primary polyclonal anti-Pc (kind gift of Renato Paro), anti-Ph or anti-GFP and HRP-conjugated secondary antibodies by chemiluminescence (Amersham Pharmacia Biotech). PABP (Roy et al., 2004), S6 (Santa Cruz Biotechnology) and eIF4A (Hernández et al., 2004) antibodies were used as loading controls. The intensities of the signals on the x-ray films were quantified on a scanning densitometer (G-710, BioRad). Optical density values were extracted and normalized to the loading controls indicated in Table 1.

Results

Characterization of the fusion proteins used in this study

As the original construct of Netter et al. (Netter et al., 2001) containing only the *UAS* promoter caused overexpression in the salivary gland nuclei, we chose to construct a *phGFP* expression vector with both a *Pc* and a *UAS* promoter (Brand and Perrimon, 1993) to better control the expression of PhGFP in embryos and larvae. The *Pc* promoter drives PhGFP expression in salivary gland nuclei at physiological levels but not in embryos and larval diploid tissues. Therefore, we used several Gal4 drivers to induce PhGFP expression in these tissues. The level of Ph is controlled by feedback inhibition of the *Ph* promoter (Fauvarque et al., 1995). The PhGFP protein was able to rescue the ph^{504}-null homozygous mutant and, thus, is totally competent in repression. PcGFP has been functionally characterized (Dietzel et al., 1999). Expression of PcGFP rescued alleles with a mutation in the Pc chromodomain (Pc^{XL5}), the domain of the protein that is essential for targeting the PcG complex by binding trimethylated lysine 27 of histone H3. In addition, the PcGFP protein binds to the same polytene chromosome loci as wild-type Pc (data not shown). However, mutations in the C-terminal region of the protein or null mutations (Pc^{2}, Pc^{3}) were not rescued. It is possible that the repression complex cannot accommodate all Pc proteins containing the GFP fusion moiety (see below) or that some other hitherto unknown aspect of Pc protein function is impaired (Dietzel et al., 1999).

Table 1. Quantification of western blots in Fig. 1

Antibody/normalized to	Relative to	Value
Polycomb/Pc^{wt}	Pc^{wt}	1
	$Pc^{wt\ in\ transgene}$	1.09
	PcGFP	0.58
Polyhomeotic/Php^{wt}	Php^{wt}	1
	Phd^{wt}	4.41
	$Php^{wt\ in\ transgene}$	2.45
	$Phd^{wt\ in\ transgene}$	3.26
	PhGFP	3.42
PhGFP/PcGFP	PcGFP	1
	PhGFP	2.2

Quantitation of western blots of imaginal discs or salivary glands from wild-type and transgenic flies revealed slightly lower levels of GFP-labeled proteins than the endogenous ones, such that the ratio of total Pc protein in transgenics (including PcGFP) was only 1.6 times that in wild type and the ratio of total Ph (including PhGFP) in transgenics was 1.7 times that of wild type (Fig. 1A,B; Table 1). PhGFP expression in wing imaginal discs was induced by Bx^{MS1096}*:Gal4* driver that induces expression in the whole wing blade. The wing blade represents 60-70% of the wing disc. Therefore, the amount of PhGFP expressed per nucleus is comparable to the amount of total untagged Ph per nucleus. There was a change in the relative expression of the proximal to the distal *Ph* genes in the transgenic line as seen in Fig. 1A. The relative expression levels of PcGFP and PhGFP in transgenic salivary glands determined by western blotting using an anti-GFP antibody was 1 to 2.2 (Fig. 1C). In the salivary gland nuclei both PcGFP and PhGFP expressions are induced by the *Pc* promoter (no Gal4 driver used in this case).

Diffusion constants of free PcGFP and PhGFP in early embryos and salivary gland nuclei

Before cellularization in *Drosophila*, the PcG proteins are all of maternal origin and their binding to chromatin is restricted to a few PRE sites (Orlando et al., 1998). It is not clear if the repression complexes formed are functional as zygotic transcription has not yet begun. Thus, there exists a window in development (early division cycles) in which one can measure the diffusion of the fusion proteins by classical FRAP techniques. In the preblastoderm embryos the distribution of PcGFP is rather homogeneous throughout the nucleus (Dietzel et al., 1999) and the nuclear size is large relative to somatic diploid nuclei later in development (Fig. 2A). At cycle 10, we observed a few faint aggregates of PcGFP in a uniform fluorescent nucleoplasm. We measured the diffusion constant in regions without aggregations by conventional FRAP. The number and intensity of the PcGFP aggregated loci increases as embryonic development proceeds and as nuclei decrease in size. Another development stage providing access to the free protein is in the larval salivary gland nuclei, where the chromatin is condensed in polytene chromosomes leaving regions of free nucleoplasm. From FRAP experiments in both early embryos (Fig. 2) and salivary gland nucleoplasm (not shown), we obtained similar diffusion constants for PcGFP of 0.74 μm^2 $second^{-1}$ and 0.41 μm^2 $second^{-1}$, respectively (Table 2). The amount of PhGFP induced in early pre-blastoderm embryos was insufficient for obtaining reproducible FRAP measurements. Thus, the free diffusion constant was derived exclusively from salivary gland nuclei. The value, 0.22 μm^2

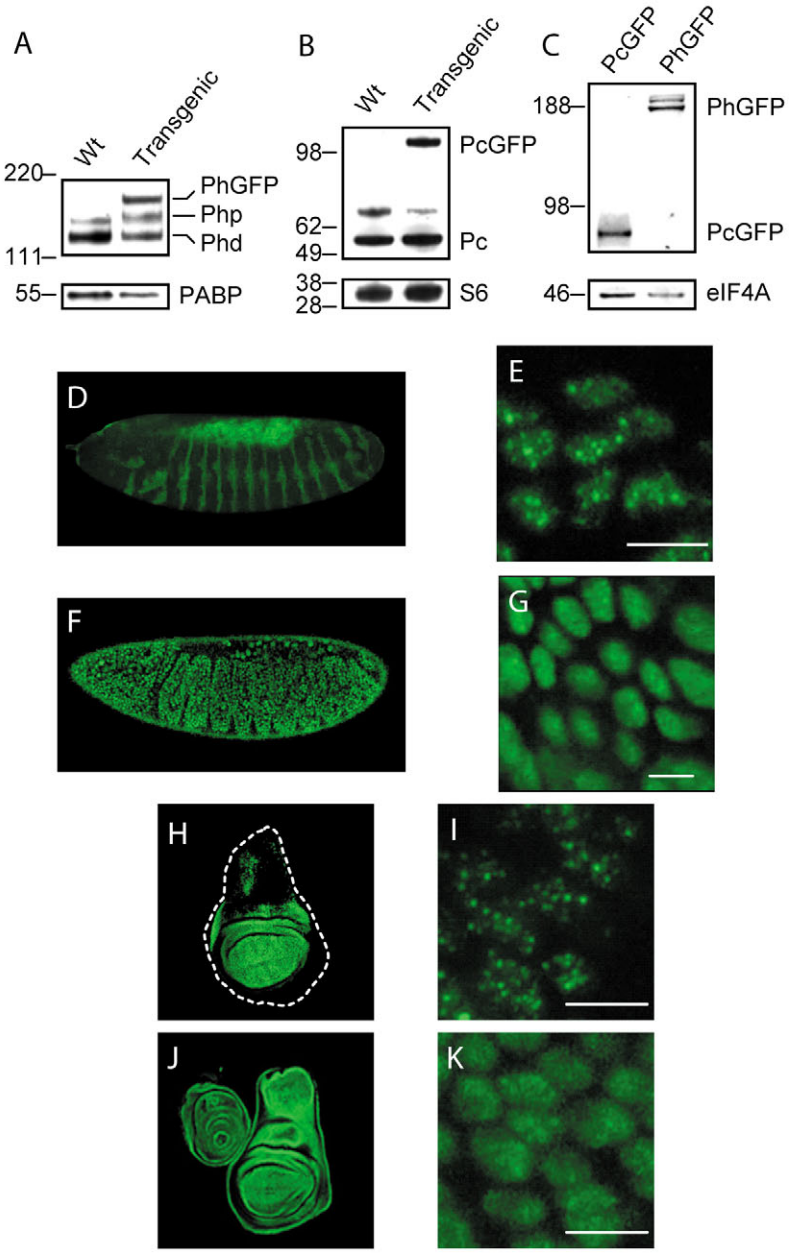

Fig. 1. Distribution patterns of PhGFP and PcGFP in the embryos and larval wing discs. (A-C) Western blot analysis of *Drosophila* tissue extracts from wild-type and transgenic fly lines. (A) Extracts from wing discs from wild-type and PhGFP-expressing larvae (probed against Polyhomeotic). (B) Extracts from wild-type and PcGFP-expressing embryos (probed against Polycomb). (C) Extracts from salivary glands from PcGFP- and PhGFP- expressing larvae (probed against GFP). Antibodies against Poly-A-binding protein (PABP) (A), S6 Ribosomal protein (B) and eIF4A (C) were used for loading control. PhGFP expression was induced using the *en:GAL4* driver in embryos (D) and the *BX*^{MS1096}*:Gal4* driver in wing imaginal discs (H). The corresponding distribution pattern of PhGFP in nuclei can be seen in E (embryos) and I (wing discs). PcGFP expression in embryos and wing imaginal discs is shown in F and J, and the respective nuclei in G and K. Scale bars: 5 μm.

second^{-1}, is only twice as slow as that of PcGFP (Table 2) as would be expected for a protein three times larger than Pc. The values for both proteins are slower than expected for free, monomeric, diffusing proteins (Verkman, 2002), indicating that the proteins may interact non-specifically in the nucleus with histones or other chromatin-bound proteins, although no specific binding to PREs occurs at this stage.

Distribution and mobility of PhGFP and PcGFP complexes in live gastrulating embryos and whole-mount imaginal discs

Our primary objective was to determine rate constants for PcG protein complexes in living embryos and tissues of *Drosophila* during stages of development when the complexes are biologically competent. Whole-mount embryos are viable and can proceed through the entire embryonic development process, i.e. through larval stages and pupation. Explanted imaginal discs cultured in vitro can develop and undergo metamorphosis by addition of hormones (Sengel and Mandaron, 1969). Thus, both embryos and imaginal discs meet our criteria for living tissue. Genetic loci are locally represented in up to 2000 copies in salivary glands, a differentiated tissue exclusive to larvae, and provide us with the possibility of observing and measuring the stability of complexes that bind to single or few PRE loci. Pc and Ph bind to overlapping target genes on these polytene chromosomes (Franke et al., 1992). After the mid-blastula transition aggregates of PcG proteins appear in all 2N nuclei of the embryo. The number of such aggregates of Ph and Pc increases during embryogenesis such that, by stage 14, over 100 such loci can be distinguished in fixed whole-mount embryos (a number similar to the number of bands observed on polytene chromosomes) (Buchenau et al., 1998). The number of distinct loci in imaginal discs is an order of magnitude smaller than in embryos, suggesting that these loci are composed of higher-order aggregates (D.J.A.-J., unpublished). The distributions of the *en:GAL4* induced PhGFP and *Pc* promoter induced PcGFP expressions in post-cellularization stages of embryogenesis and in wing imaginal discs are shown in Fig. 1D-K.

As shown in the following sections, the recovery times of the PcGFP and PhGFP complexes were at least an order of magnitude longer than the free diffusion of the macromolecules. Thus, it was necessary to measure for more than 50 seconds in order to reach equilibrium between the redistribution of bleached and unbleached proteins. A preferred method for determining dissociation rate constants under such conditions is to use inverse FRAP (iFRAP), whereby the entire nucleus (except for a small region surrounding the fluorescent complex of interest) is bleached and the depletion of fluorescence from this region is monitored over time. The rate of disappearance of the fluorescent locus will be a direct measure of the first order dissociation rate constant of the protein from the complex (Dundr et al., 2002). We found that this type of photobleaching technique fitted our system best due to the reasons described below. Nuclei and chromatin itself are not

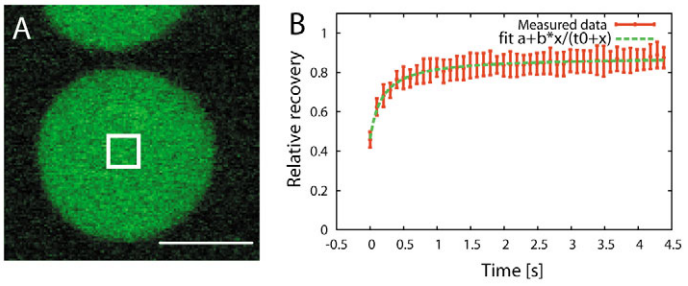

Fig. 2. Diffusion of PcGFP in nuclei of preblastoderm embryos. A square-shaped region (1.5×1.5 μm) in the center of a preblastoderm nucleus (A) of a PcGFP embryo was photobleached and the fluorescence recovery was measured over time. (B) Data points for 40 FRAP curves from similar nuclei as in (A) were averaged and fitted to a hyperbolic function (Eqn 2 in the Materials and methods). Scale bar: 5 μm.

stationary in live *Drosophila* tissues, as shown in Fig. 3. Core histone-GFP that does not dissociate from chromatin in interphase showed similar dynamics, indicating that the movement we observe in our cells is not due to dissociation of whole complexes from the chromatin (Post et al., 2005) (see Movie 1 in the supplementary material). In addition, photobleaching of the nuclear lamin fused to RFP in embryonic and 2N larval disc *Drosophila* nuclei revealed no rotation of

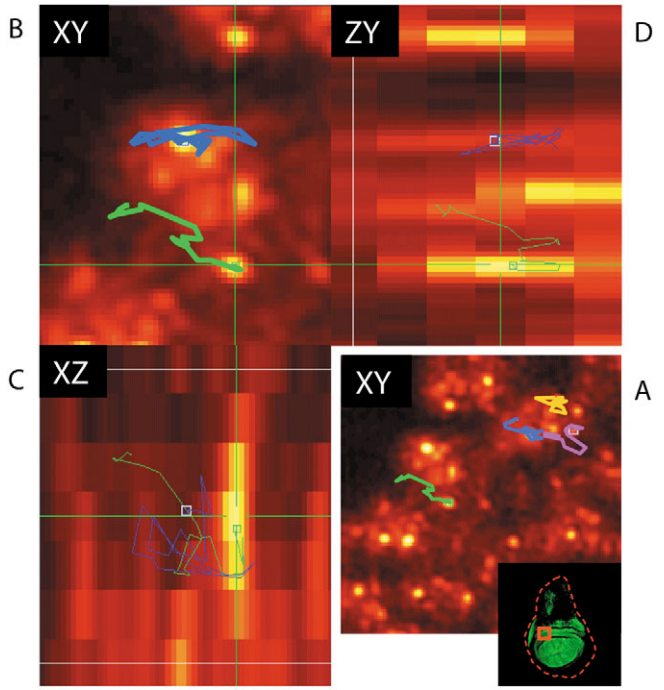

Fig. 3. Chromatin dynamics in diploid nuclei. (A) Inset: fluorescence image of a PhGFP larval wing disc. Intensity pseudo-colored magnified image of the region boxed in the inset. A stack of seven *z*-sections was imaged repeatedly at 5-second intervals for 120 seconds. Time traces of several loci are indicated by the colored tracks. (B) A single XY plane at time 0 from the stacks is displayed. Time XY tracks are superimposed for two loci (blue and green traces). Zero time (C) XZ planes and (D) ZY planes for the slices designated by the cross-hair in image B. Time traces for the positions of the two loci are superimposed showing the large movements.

Table 2. Diffusion constants for PhGFP and PcGFP

	Preblastoderm embryos	Salivary gland nuclei
PCGFP	D=0.74 μm^2/second	D=0.41 μm^2/second
PHGFP		D=0.22 μm^2/second

the nuclei over a period of more than 3 minutes (C. Fritsch, personal communication). In order to overcome the problem of chromatin mobility, the dissociation and residence times of the PcG chromatin-bound proteins were analyzed in three dimensions by adapting the iFRAP procedure to a version denoted 3D-iFRAP that tracks the fluorescent locus over time (see Materials and methods). The fluorescence decay of the unbleached locus and the increase in fluorescence in the bleached nucleus were monitored in the movement corrected data (Fig. 4) and the average intensities of the locus of interest were plotted over time to derive the rate constants (Fig. 5).

Dissociation rate constants of PcG complexes in nuclei of embryos and imaginal discs

3D-iFRAP was used to analyze the residence times and dissociation rate constants of PcG fusion proteins in embryo and wing imaginal disc nuclei of PcGFP- and PhGFP-expressing flies (Fig. 5). Individual recovery times for PhGFP loci in stage 13 to 16 embryos showed a Gaussian distribution

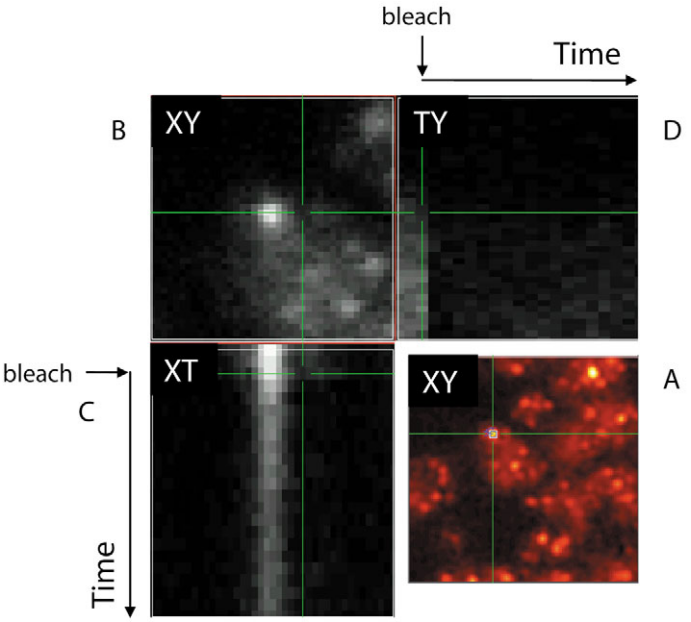

Fig. 4. 3D-iFRAP. (A) Overview of part of a wing disc with cross-hair on the fluorescent locus selected for iFRAP. Fluorescence depletion was calculated from a recorded series of *z*-stack images over time after bleaching and image registration. (B) Magnified XY confocal image of the nucleus before bleaching. Cross-hair set in the bleach region next to the unbleached locus. The images have been registered to correct for the movement of the chromatin, and the nucleus itself and the fluorescent locus is centered in the final analysis image time stack. (C,D) X-time and time-Y views, respectively, of the registered images at the slices in the XY image corresponding to the cross-hair in B. In C, dissociation of the fluorescent molecules from the spared locus can be seen over time. In D, a bleached region is shown over time. The transition from before bleaching to after bleaching is indicated by the arrows in the time planes.

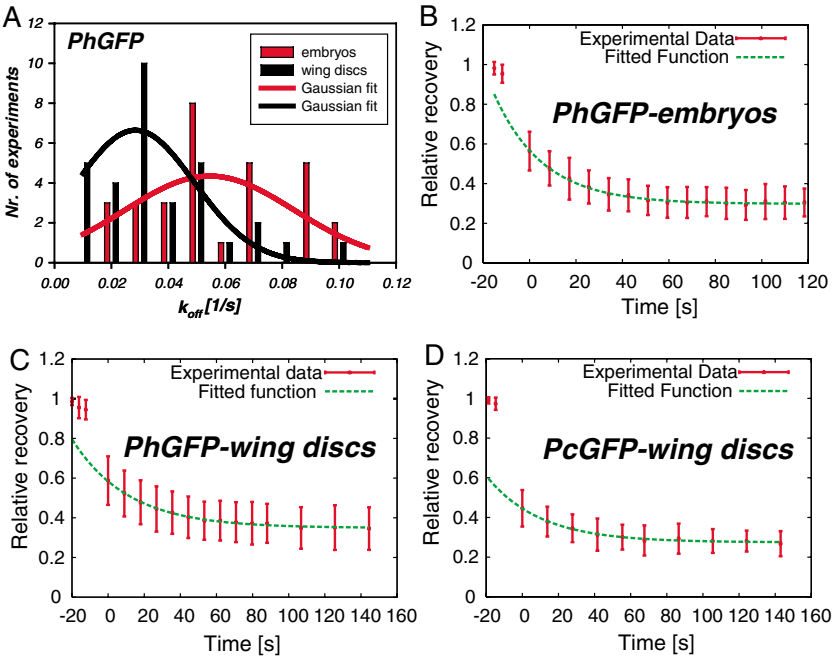

Fig. 5. Dissociation rate constants for PhGFP and PcGFP. Individual PcG protein loci in the diploid nuclei of the embryos and wing imaginal discs were subjected to 3D-iFRAP. Fluorescence decay curves were fitted to a single exponential function. (A) Histogram of dissociation rate constants of individual PhGFP loci obtained from 3D-iFRAP experiments in embryos and larval wing imaginal discs are shown in red and black, respectively. (B) A single dissociation rate constant could be fitted by averaging all 30 normalized data from PhGFP embryos (k_{off}=0.051±0.004 second^{-1}). (C) Average of all 32 normalized data from PhGFP wing discs (k_{off}=0.032±0.002 second^{-1}). (D) Average dissociation rate curve for data from 10 determinations of PcGFP loci in imaginal discs (k_{off}=0.034±0.003 second^{-1}).

around 20 seconds (Fig. 5A). Thus, we fit a single exponential decay function to the average data from 30 measurements after normalization to the initial intensities (see Fig. 5B). Such a procedure resulted in a single dissociation rate constant of k_{off}=0.051±0.004 second^{-1} in embryos. In wing imaginal disc nuclei of PhGFP-expressing flies, we found a similar distribution of dissociation rate constants, although with a slightly positive skewness (Fig. 5A). Averaging 32 individual curves, we fit a single dissociation rate constant of k_{off}=0.032±0.002 second^{-1} (Fig. 5C).

Although both PcGFP and PhGFP are localized similarly to 30-40 loci in imaginal disc nuclei, the fraction of free fusion protein differs for the two fusion proteins, as seen in Fig. 1. The iFRAP method requires the complete photo-destruction of all free protein, which results in some unintended collateral bleaching of the fluorescent locus of interest by the high NA objective used in the case of PcGFP nuclei that contain a large amount of free protein, as seen by comparing the pre-bleach and first post bleach intensity measurements in Fig. 5B-D. The reduced fluorescence intensity in the complex decreased the signal to noise ratio for the measurement and reduced the accuracy of the determination of the dissociation rate constant. We compensated for this problem by performing a global fit on all of the dissociation curves for all experiments from the wing discs for the PcGFP. From the dissociation curve depicted in Fig. 5D, a dissociation rate constant of k_{off}=0.034±0.003 second^{-1} was determined, very similar to the dissociation rate constant of PhGFP in larval disc nuclei.

PcG complexes have different residence times on individual bands in salivary gland nuclei

PcGFP and PhGFP bind to distinct (Fig. 6) overlapping loci in salivary gland nuclei. Classical FRAP experiments (intense photobleaching of the band and monitoring of the fluorescence recovery over time) (Fig. 6E) were conducted on individual bands to determine the dissociation rate constants for PcGFP and PhGFP complexes. Individual bands showed consistent recovery times after multiple bleachings (Fig. 6F), although not all bands in the same nucleus exhibited the same recovery times (Fig. 6B,D). The equilibrium association constant of the complex is given by the ratio of a pseudo first-order forward rate constant (which includes the concentration of the free protein) and a first-order dissociation rate constant. In the case of PcGFP, a large amount of the labeled protein is free, i.e. leading to a lower fraction of bound protein than for PhGFP (bound ratio, B_{ratio}, see Materials and methods, Fig. 8B). Therefore, the shape of the FRAP recovery curve will be dominated by the fast diffusion of the free protein, as is evident from the comparison of the curves in Fig. 6B,D. We accounted for the free protein component by segmenting out the bound fraction of proteins from the bleach box (Fig. 7) (as described in the Materials and methods, and further explained in the Discussion). A comparison of the recovery curves for the bound fraction (blue curve) and the unbound free component (green curve) of PhGFP and PcGFP (Fig. 7D,F) shows that the segmentation separated the fast recovery process of the free protein (which occurs in the first seconds) from the actual binding reaction. By fitting the recovery curve for the bound fraction, we computed recovery times (t_0, the time required for the fluorescence intensity to reach ~63% of the final height of the recovery curve for the bound molecules) for both PhGFP and PcGFP from such curves (Fig. 8A). The distribution of values was very similar for both proteins with t_0 recovery times ranging from 50 to 350 seconds.

In the case of salivary gland polytene chromosomes, the individual bands represent complexes binding to one or a few genes. Thus, we can ask if the range of measured recovery times represents different exchange rates for different genes (PREs) or the same exchange rate influenced by the density of binding sites. Simulations revealed that for interpreting these FRAP experiments the complex interplay between unbleached free protein, the total amount of bound protein at a locus and the free diffusion constant must be taken into account. We simulated the expected FRAP behavior for loci with different

amounts of bound protein at a locus (thus different intensities), as briefly described in the Materials and methods, using a diffusion constant of 0.5 μm^2 second^{-1} of the free protein determined experimentally and by systematically varying the dissociation rate constants around the experimentally determined values (a complete description of the simulations will be presented elsewhere). Fig. 8B demonstrates that with a single dissociation rate constant we would expect the recovery times to vary approximately linearly with the ratio of bound to free protein, B_{ratio}, as defined in the Materials and methods, Eqn 5, and results in the data shown by the connected points. In Fig. 8B, the experimentally measured recovery times are also plotted against the B_{ratio} for each locus. In the experimental data, no strong correlation was found between the recovery time and the intensity of the locus (number of binding sites), indicating that the complexes on different genes have different stabilities, and implying that they differ in composition. Including the dependence of the dissociation time on the density of binding sites, B_{ratio}, and the free diffusion component (determined experimentally to be ~0.5 μm^2 second^{-1}) as predicted from the simulations, we calculated dissociation rate constants for each of the analyzed loci using Eqn 6. These values are independent of the local concentration of sites and the effect of diffusion. Bound protein ratios were normalized to the highest B_{ratio} value for each protein separately and are plotted in Fig. 9A. The dissociation rate constants are similar for both proteins but about one-fifth the values found for the complexes in 2N wing disc nuclei. The forward reaction is 2nd order and the rate is dependent on the concentration of binding sites and on the local concentration of the free protein. The amount of unbound protein in the nucleus is sufficient for the binding process to occur undisturbed for both PhGFP and PcGFP cases. From the fluorescence intensity ratios, we calculated that ~10% of the total PhGFP and ~2% of the PcGFP are in a bound state in a salivary gland nucleus at equilibrium. As the absolute number of binding sites (C_s) is unknown, the association rate constant could not be determined independently. Instead, a pseudo-association rate constant was calculated (which is related to the actual k_{on} by the equality $k_{on}^*=k_{on}\cdot C_s$, see Materials and

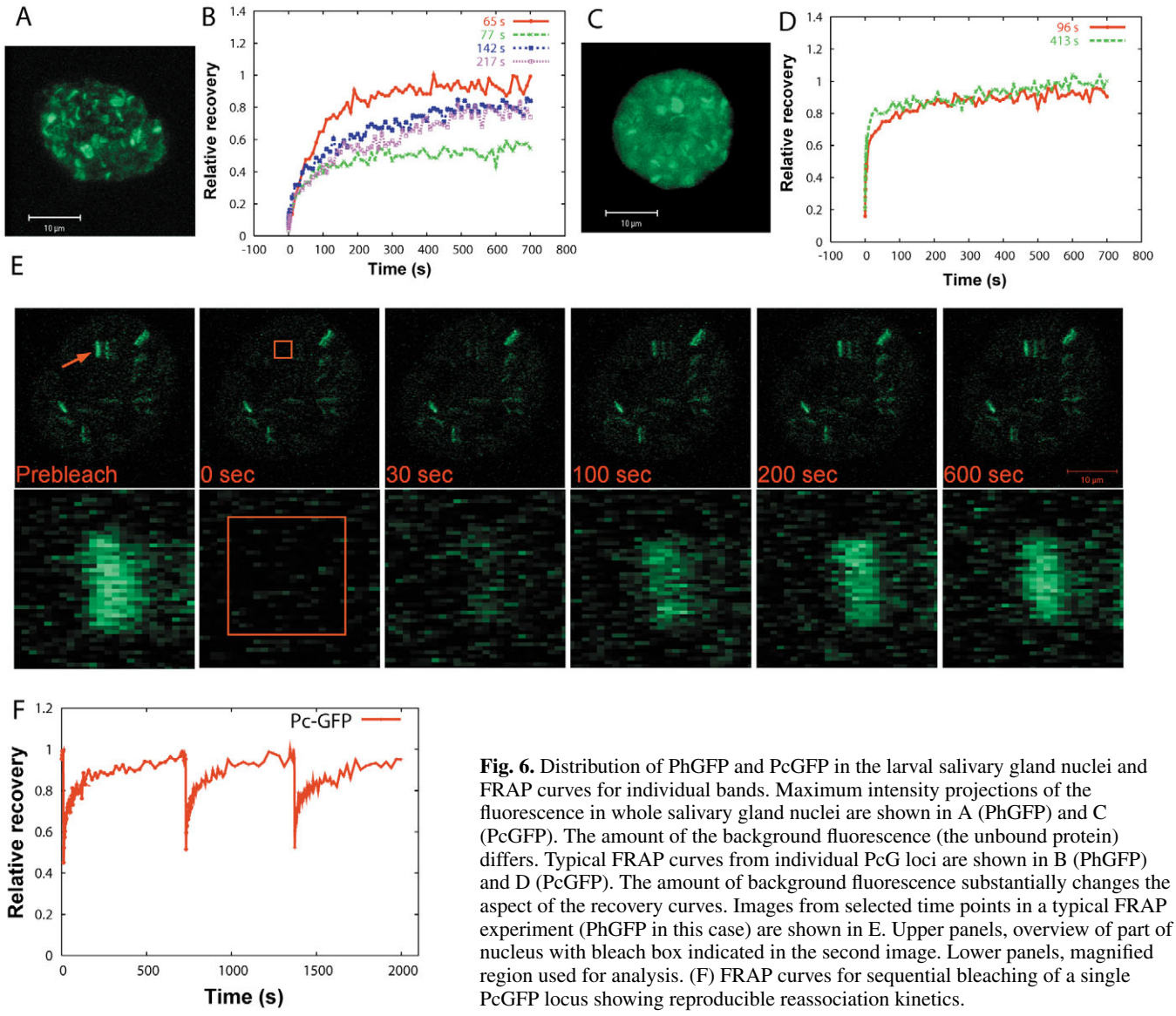

Fig. 6. Distribution of PhGFP and PcGFP in the larval salivary gland nuclei and FRAP curves for individual bands. Maximum intensity projections of the fluorescence in whole salivary gland nuclei are shown in A (PhGFP) and C (PcGFP). The amount of the background fluorescence (the unbound protein) differs. Typical FRAP curves from individual PcG loci are shown in B (PhGFP) and D (PcGFP). The amount of background fluorescence substantially changes the aspect of the recovery curves. Images from selected time points in a typical FRAP experiment (PhGFP in this case) are shown in E. Upper panels, overview of part of nucleus with bleach box indicated in the second image. Lower panels, magnified region used for analysis. (F) FRAP curves for sequential bleaching of a single PcGFP locus showing reproducible reassociation kinetics.

methods, Eqn 7) (Sprague et al., 2004) for each locus and these values for PhGFP are plotted in Fig. 9B. The pseudo-association rate constants are an order of magnitude larger than the dissociation rate constants, confirming that dissociation is rate limiting.

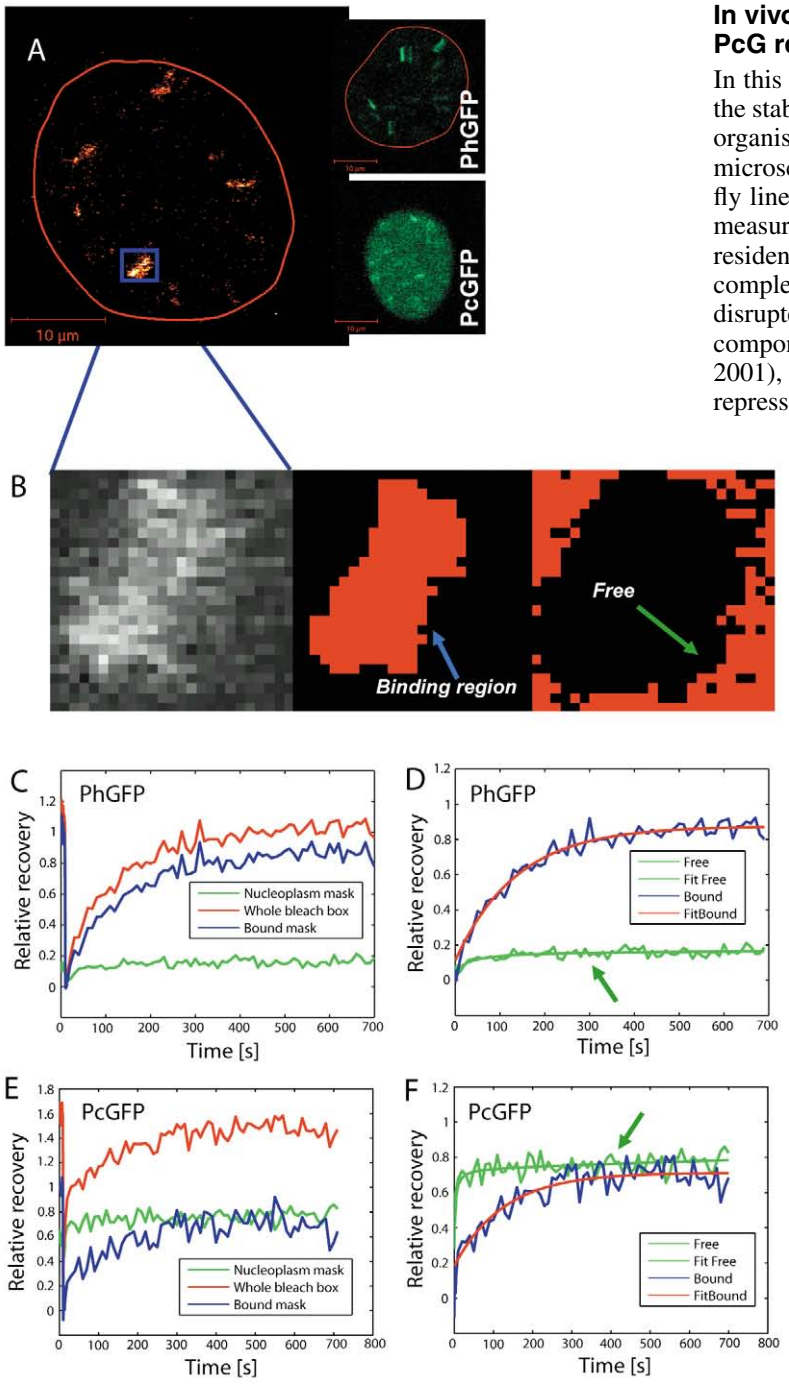

Fig. 7. Segmentation of the bound fraction and fitting of the FRAP curves. A confocal image of PhGFP in a salivary gland nucleus is shown in A. Inset: confocal sections for PhGFP and PcGFP salivary gland nuclei. (B) Segmentation of the bleach box area into bound and unbound fluorescence regions. (C,E) Plot of the intensity for all pixels (red curve), the 30% highest pixels, bound fraction (blue curve) and the 30% lowest pixels (green curve). (C) PhGFP. (E) PcGFP. (D,F) Fit of the bound fraction of the protein to a single exponential (blue curve). The height of the green curve (unbound component) differs for PhGFP and PcGFP. (D) PhGFP. (F) PcGFP.

Discussion

In vivo experiments to investigate the stability of PcG repression complexes

In this paper, we have addressed fundamental questions about the stability and lifetime of PcG repression complexes in living organisms on their target sites. Applying photobleaching microscopy and computer modeling to transgenic *Drosophila* fly lines expressing GFP fused PcG proteins, we were able to measure diffusion constants, dissociation rate constants and residence times of PcG complexes on chromatin. Although complexes of PcG proteins have been isolated in vitro from disrupted cells (Saurin et al., 2001) or assembled from protein components expressed in heterologous systems (Francis, 2001), none of these in vitro systems recapitulates the actual repression mechanism occurring in host organisms. That is, specific binding to PREs and gene-specific repression have not been demonstrated in vitro. The in vitro experiments showing chromatin binding and interference with remodeling machines or transcription complexes demonstrated that individual members of the PRC1 could produce similar interference as the complete complex in some cases (Francis et al., 2004). Repression occurred on chromatin consisting of nucleosomes without histone tails (Shao et al., 1999), results that do not recapitulate the in vivo situation. Removal of cis-acting Polycomb repressor elements (PRE) in vivo even at later developmental stages leads to derepression of homeotic genes (Busturia et al., 1997), indicating that propagation of the silenced state requires the activity of proteins that bind directly to the PREs and not to chromatin in general. In fact, in the organism, deficiency in single PcG genes causes loss of function (Beuchle et al., 2001) and targeting of PcG complexes requires trimethylation of lysine 27 of histone H3 (Cao et al., 2002; Müller et al., 2002). The discrepancy between in vitro and in vivo repression may be the result of non-physiological conditions for the binding and inhibition experiments. A further complication is the fact that there is evidence of in vivo hierarchical assembly on chromatin (Wang et al., 2004), whereas in vitro complexes are preformed and bound to chromatin. To avoid these problems, we chose to address the question of the stability of PcG complexes in live animals and tissues. Our results indicate that the repression system is flexible and based on a continuous exchange of the PcG members at specific loci in the genome.

Quantitative FRAP and 3D-iFRAP

The application of fluorescence recovery after photobleaching (FRAP) to fusion proteins of GFP (and its analogs) by confocal microscopy has allowed the study of the dynamics of the steady-state distribution of nuclear proteins in living cells (Houtsmuller and Vermeulen, 2001; Phair and

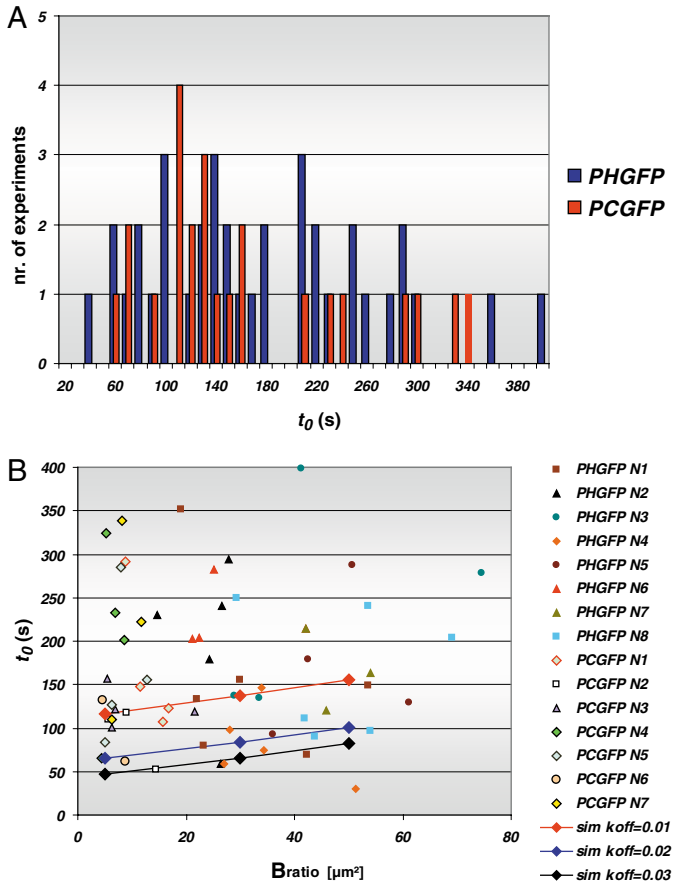

Fig. 8. FRAP on bound PcG proteins in the salivary gland nuclei. Individual bands in the salivary gland nuclei were photobleached and redistribution of fluorescence was measured over time. Recovery times (t_0, the time required for the fluorescence intensity to reach ~63% of the final height of the recovery curve) were plotted as a histogram in A (blue, PhGFP; red, PcGFP). Redistribution of the fluorescence in both cases occurs in less than 6 minutes. (B) Lack of correlation between the concentration of binding sites and recovery time t_0. Individual nuclei where several loci were analyzed are color coded (solid colored symbols for PhGFP and open colored symbols for PcGFP). Data from simulations show a linear dependence of the t_0 on the concentration of binding sites (connected points for three different dissociation rate constants).

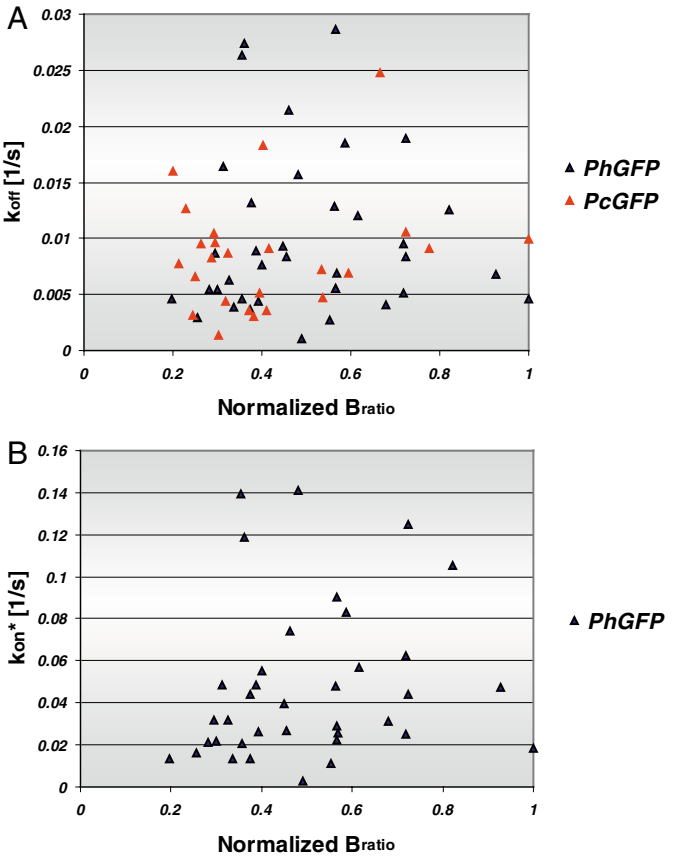

Fig. 9. Dissociation rate constants for PhGFP and PcGFP and reassociation rate constants for PhGFP. (A) Dissociation rate constants for PhGFP (blue) and PcGFP (red) plotted against the normalized concentration of binding sites for individual loci. (B) Pseudo-reassociation rate constants for PhGFP (blue). See text for details.

Misteli, 2001; White and Stelzer, 1999). Although most analyses have been qualitative (Cheutin et al., 2003; Dou et al., 2002; Festenstein et al., 2003; Houtsmuller et al., 1999; McNally et al., 2000; Misteli et al., 2000), a quantitative analysis can be used to obtain diffusion constants and dissociation rate constants by the application of combined techniques and appropriate models (Carrero et al., 2003; Dundr et al., 2004; Dundr et al., 2002; Phair et al., 2004; Rabut, 2004). In most cases, however, a reaction dominant model has been adopted. That is, because diffusion is faster than most dissociation rates, it is often, albeit incorrectly, neglected in the analyses. Recently, Sprague et al. presented a full analytical treatment for uniformly dispersed binding sites and showed simulations for various boundary conditions and rate constants (Sprague et al., 2004). Because our complexes are not uniformly distributed we have extended this treatment to a model with discrete binding loci and present here simulations using diffusion and binding rate constants derived from our experimental data. (A full description of the model will be presented elsewhere.)

Our FRAP experiments are somewhat different from those presented previously in the literature. We used live whole animals and tissues, rather than adherent tissue culture cells. This fact required adaptation of the acquisition method to include 3D tracking of loci after inverse FRAP bleaching (3D-iFRAP) as *Drosophila* diploid cells show an extensive reorganization of nuclear content during measurement times in the minute range (see Fig. 3 and see Movie 1 in the supplementary material) (Post et al., 2005). After registration of the fluorescent locus over time, we were able to calculate the dissociation rate constants for PcG complexes in embryos and imaginal discs. We found very consistent and similar behavior for both proteins in the complexes in the wing discs, corresponding to dissociation rate constants of 0.032±0.002 second^{-1} for PhGFP and 0.034±0.003 second^{-1} for PcGFP (Figs 4 and 5), slightly smaller than in embryos for which the dissociation rate constant for PhGFP was 0.051±0.004 second^{-1}. All of these complexes were completely exchanged in less than 3 minutes. That is, both PcGFP and PhGFP in PcG complexes in vivo exchanged in an order of magnitude shorter time than the cell cycle. These data rule out a model for

repression by which PcG complexes would mask the chromatin and render it inaccessible to transcription factors or other proteins as we discuss below.

The influence of diffusion and free protein on FRAP data and binding equilibria

The level of Pc is crucial for the maintenance of a competent complex as can be deduced from the fact that $Pc^{+/-}$ heterozygotes show homeotic transformations (Lewis, 1978). Western blotting revealed that the fusion proteins do not reach levels greater than the wild type in non-transgenic animals (Table 1). That is, the total PcGFP protein content in the mutants was 0.53 that of wild type and PhGFP was comparable with the wild-type level.

The diffusion constants for PcGFP in early embryos before complex formation (0.74 μm^2 $second^{-1}$) and in the nucleoplasm of salivary gland nuclei (0.41 μm^2 $second^{-1}$) are smaller than one might expect for a protein of ~62 kDa, indicating that the protein may exhibit non-specific binding to chromatin. Breiling et al. (Breiling et al., 1999) demonstrated that Pc has an affinity for nucleosomes without histone tails and that the C terminus was crucial for this interaction. However, the Pc chromodomain, essential for complex assembly, has a strong preference for trimethylated Lys 27 over other methylated sites or unmodified H3 showing a K_D of 5 μM and >1000 μM, respectively, in in vitro binding studies (Fischle, 2003). As seen in Fig. 6, the diffusion of the free protein obscures the recovery kinetics of the binding process measured on individual bands in salivary glands and the curve must be decomposed to fit the recovery kinetics (Fig. 7). The fitting assumes an excess of free protein, which is true for both of our transgenic proteins, despite the lower nucleoplasmic fluorescence in the case of PhGFP (see below). In an ideal situation with infinitely fast diffusion, loci with different concentrations of binding sites of identical affinity would recover within the same time. At the diffusion constants measured experimentally in our nuclei (~0.5 μm^2 $second^{-1}$), we found by simulation that two loci with the same size but with different concentrations of binding sites will recover with different times: i.e. higher concentration, longer recovery time (Fig. 8). We created masks in the images to separate out pixels that contained predominantly non-bound protein from that involved in complexes. By first fitting and removing the diffusion component we were able to fit the resulting recovery curves to a single exponential, as in a kinetic process in a standard chemical equilibrium (Fig. 7). The dissociation rate constants were in the same range as those measured in the 2N cells of embryos and imaginal discs but the means were shifted towards a value of around one-third of that for PhGFP to one-quarter of that for PcGFP. These differences could reflect some unintended bias in the selection of the bleach loci in either the 2N nuclei or the polytene bands. However, each polytene band represents thousands of complexes at one or a few PREs, rather than an average of many different complexes; thus, these data may be more robust. In either case, even when PREs are in close proximity, such as is the case of a thousand chromatids closely aligned in the polytene chromosomes, the PcG proteins are in a chemical equilibrium with unbound protein. The reduced rate constants may reflect the large local binding sites, whereby a dissociated protein does not immediately join the 'free pool' but has a higher probability to rebind in the close vicinity. However, the proteins are not 'trapped' in the complex but rather are able to completely exchange in under 6 minutes. The reproducibility of the recovery times of individual bands subjected to successive FRAP measurements is shown in Fig. 6F, indicating that the differences of two- to threefold in recovery times (Fig. 8) between different bands can be considered reproducible and significant.

The t_0 values calculated from these recovery curves are, however, not a direct measure of residence time because of their dependence on the effect of diffusion transport in combination with ongoing depletion from the free pool. As could be demonstrated using simulations, if the dissociation rate constant and the concentration of free protein were the same for all complexes then one would expect the recovery rate to depend linearly on the amount of bound protein (lines in Fig. 8B), which is essentially a measure of the ability of a spot to deplete the free protein pool during recovery. As seen in the same figure, the experimental data do not show such a correlation, implying that there are differences in the composition of the complexes on different genetic loci and that the dissociation rate constants, though similar (within a factor of 5, Fig. 9A), reflect the specific mixture of PcG and non-PcG auxiliary proteins on the polytene bands. Such an interpretation is compatible with the data of Rastelli et al., who showed varying occupancy of PcG proteins and Zeste on more than 100 bands by immunohistochemistry on polytene chromosomes (Rastelli et al., 1993). To rule out the possibility of a very slow component that would appear as an immobile fraction in a single exponential fit, we also fitted the data with a sum of two exponentials, but did not find a consistent second time in this case and less precision of the first time. Thus, we conclude that both PcGFP and PhGPF in repression complexes exchange within a few minutes in live *Drosophila* cells.

In Fig. 9B, the pseudo-association rate constants as described in the Materials and methods are plotted for PhGFP. The values are an order of magnitude larger than the dissociation rate constants and thus, dissociation is rate-limiting. We have not attempted to present pseudo-association rate constants for PcGFP for the following reasons. We assume that the number of binding sites for Pc and Ph are approximately equal as the proteins bind to overlapping sites on polytene chromosomes (Rastelli et al., 1993), isolated complexes of the proteins contain equimolar quantities of both proteins (Saurin et al., 2001) and they are targeted to the same PREs by ChIP analysis (Breiling et al., 2001). As discussed above, the off-rates are similar for the two proteins. However, we can see a larger pool of unbound PcGFP compared with PhGFP in both embryos and larval tissue (Figs 1 and 6). As determined from western blots in salivary glands, PcGFP is not present in amounts higher than PhGFP (Fig. 1C). Wang et al. (Wang et al., 2004) have shown that there is sequential recruitment of PcG complexes to the PREs, whereby Pc targets the complex to chromatin by binding to trimethylated H3K27 (Cao et al., 2002; Czermin et al., 2002; Fischle et al., 2003; Wang et al., 2004). From these considerations, we postulate that the PcGFP fusion protein, although competent to target PREs with modified histones and engage in a competent complex, cannot substitute for all Pc molecules in the complexes (perhaps owing to steric hindrance of adjacent GFP moieties). Our data suggest that the unmodified Pc is preferred in the complex by a factor of about 4 or 5; thus, association

rate constants calculated for PcGFP will not properly reflect the true on rate of the unmodified protein, whereas off rates should not be adversely affected.

We calculated the ratio of the bound/free fusion proteins from the segmentation of the salivary gland prebleach FRAP images to be 1:10 and from the western blots (Fig. 1) the ratio of the fusion protein to wild-type protein of 1:1. We estimated the absolute concentration of GFP protein in the salivary gland nuclei to be ~2-4 μM by comparison to the intensity of droplets of purified GFP protein in an immiscible solution in our microscope system. If the total concentration of binding sites is equivalent to the concentration of the bound Ph, we can estimate the K_D for the protein in vivo in salivary gland nuclei to be ~5 μM.

Conclusions

Using photobleaching in confocal microscopy and computer simulations, we determined the stability of PcG protein complexes during development. These are the first FRAP experiments performed in whole live organisms and tissues. We found that all complexes were exchangeable throughout all developmental stages. The relatively short residence times of 2-6 minutes for Ph and Pc in the repression complex rule out models for repression that invoke blocking chromatin access. They also suggest that competition could exist between antagonistic factors at PREs and promoters, allowing modulation of the state of repression during development by changes in their balance. These data complement those found in other systems, such as the direct competition for chromatin binding sites between histone H1 and microinjected high-mobility group (HMG) proteins, as demonstrated by Catez et al. (Catez et al., 2004).

Most FRAP studies of nuclear proteins have involved components in transcription complexes or transcriptional activators that exchange in less than 2 minutes (Phair et al., 2004). The only repressor protein that has previously been investigated is heterochromatin protein 1 (HP1), a protein targeted to heterochromatin in higher eukaryotes (Cheutin et al., 2003; Festenstein et al., 2003). Although HP1 is loaded directly onto the chromatin during replication, it was found by FRAP to bind only transiently to chromatin with a maximum residence time of ~60 seconds. Thus, both HP1 and PcG repression complexes appear to function by dynamic competition with other chromatin-binding proteins rather than by formation of a static, higher-order chromatin structure with immobilized bound repressors. Our FRAP measurements on polytene chromosomes revealed differences in the dissociation rate constants between individual bands that imply a flexible repression system of complexes with various compositions that influence the binding affinity of other members and whose turnover is in the order of a few minutes.

We conclude that: (1) activation and repression can be dynamically controlled by simple chemical equilibria; (2) reduction in PcG levels will facilitate epigenetic change and may explain why non-cycling cells can be reprogrammed more easily than cycling cells (Baxter et al., 2004); and (3) PcG complexes are exchangeable protein assemblies that maintain repression over many cell cycles by simple chemical equilibria.

We thank C. Fritsch for extensive constructive discussions and editorial assistance with the manuscript; G. Hernández for antibodies, help and advice; J. Müller for plasmids; and . Jäckle, R. Paro and F. Netter for fly strains and plasmid constructs. We are also grateful to T. Jovin for suggestions in the experimental design, and for discussions and assistance with FRAP analysis and equilibrium kinetics. The work was supported by a Max Planck Predoctoral Fellowship to G.F. This work is part of the scientific research conducted in the International PhD Program Molecular Biology-International Max Planck Research School at the Georg August University (Göttingen, Germany).

References

Baxter, J., Sauer, S., Peters, A., John, R., Williams, R., Caparros, M. L., Arney, K., Otte, A., Jenuwein, T., Merkenschlager, M. and Fisher, A. G. (2004). Histone hypomethylation is an indicator of epogenetic plasticity in quiescent lymphocytes. *EMBO J.* **23**, 4462-4472.

Beuchle, D., Struhl, G. and Muller, J. (2001). Polycomb group proteins and heritable silencing of *Drosophila* Hox genes. *Development* **128**, 993-1004.

Bienz, M. and Muller, J. (1995). Transcriptional silencing of homeotic genes in *Drosophila*. *BioEssays* **17**, 775-784.

Brand, A. H. and Perrimon, N. (1993). Targeted gene expression as a means of altering cell fates and generating dominant phenotypes. *Development* **118**, 401-415.

Breiling, A., Turner, B., Bianchi, M. and Orlando, V. (2001). General transcription factors bind promoters repressed by Polycomb group proteins. *Nature* **412**, 651-655.

Breiling, A., Bonte, E., Ferrari, S., Becker, P. B. and Paro, R. (1999). The Drosophila Polycomb protein interacts with nucleosomal core particles in vitro via its repression domain. *Mol. Cell. Biol.* **19**, 8451-8460.

Breiling, A., O'Neill, L. P., D'Eliseo, D., Turner, B. M. and Orlando, V. (2004). Epigenome changes in active and inactive polycomb-group-controlled regions. *EMBO Rep.* **5**, 976-982.

Buchenau, P., Hodgson, J., Strutt, H. and Arndt-Jovin, D. J. (1998). The distribution of polycomb-group proteins during cell division and development in Drosophila embryos: impact on models for silencing. *J. Cell Biol.* **141**, 469-481.

Busturia, A. and Morata, G. (1988). Ectopic expression of homeotic genes caused by the elimination of the Polycomb gene in *Drosophila* imaginal epidermis. *Development* **104**, 713-720.

Busturia, A., Wightman, C. D. and Sakonju, S. (1997). A silencer is required for maintenance of transcriptional repression throughout *Drosophila* development. *Development* **124**, 4343-4350.

Cao, R., Wang, L., Wang, H., Xia, L., Erdjument-Bromage, H., Tempst, P., Jones, R. S. and Zhang, Y. (2002). Role of histone H3 lysine 27 methylation in Polycomb-group silencing. *Science* **298**, 1039-1043.

Capdevila, J. and Guerrero, I. (1994). Targeted expression of the signaling molecule Decapentaplegic Induces pattern duplications and growth alterations in Drosophila wings. *EMBO J.* **13**, 4459-4468.

Carrero, G., McDonald, D., Crawford, E., de Vries, G. and Hendzel, M. J. (2003). Using FRAP and mathematical modeling to determine the in vivo kinetics of nuclear proteins. *Methods* **29**, 14-28.

Catez, F., Yang, H., Tracey, K. J., Reeves, R., Misteli, T. and Bustin, M. (2004). Network of dynamic interactions between histone H1 and high-mobility-group proteins in chromatin. *Mol. Cell. Biol.* **24**, 4321-4328.

Chan, C. S., Rastelli, L. and Pirrotta, V. (1994). A Polycomb response element in the Ubx gene that determines an epigenetically inherited state of repression. *EMBO J.* **13**, 2553-2564.

Cheutin, T., McNairn, A. J., Jenuwein, T., Gilbert, D. M., Sihgh, P. B. and Misteli, T. (2003). Maintanance of stable heterochromatin domains by dynamic HP1 binding. *Science* **299**, 721-725.

Chiang, A., O'Connor, M. B., Paro, R., Simon, J. and Bender, W. (1995). Discrete Polycomb-binding sites in each parasegmental domain of the bithorax complex. *Development* **121**, 1681-1689.

Czermin, B., Melfi, R., McCabe, D., Seitz, V., Imhof, A. and Pirrotta, V. (2002). *Drosophila* Enhancer of Zeste/ESC complexes have a histone H3 methyltransferase activity that marks chromosomal polycomb sites. *Cell* **111**, 185-196.

Dellino, G. I., Schwartz, Y. B., Farkas, G., McCabe, D., Elgin, S. C. R. and Pirrotta, V. (2004). Polycomb silencing blocks transcription initiation. *Mol. Cell* **13**, 887-893.

Dietzel, S., Niemann, H., Brückner, B., Maurange, C. and Paro, R. (1999). The nuclear distribution of Polycomb during *Drosophila melanogaster* development shown with a GFP fusion protein. *Chromosoma* **108**, 83-94.

Dou, Y., Bowen, J., Liu, Y. and Gorovsky, M. A. (2002). Phosophorylation

and an ATP-dependent process increase the dynamic exchange of H1 in chromatin. *J. Cell Biol.* **158**, 1161-1170.

Dundr, M., Hoffmann-Rohrer, U., Hu, Q., Grummt, I., Rothblum, L. I., Phair, R. D. and Misteli, T. (2002). A kinetic framework for a mammalian RNA polymerase in vivo. *Science* **298**, 1623-1626.

Dundr, M., Herbert, M. D., Karpova, T. S., Stanek, D., Xu, H., Shpargel, K. B., Meier, U. T., Neugebauer, K. M., Matera, A. G. and Misteli, T. (2004). In vivo kinetics of Cajal body components. *J. Cell Biol.* **164**, 831-842.

Fauvarque, M. O., Zuber, V. and Dura, J. M. (1995). Regulation of polyhomeotic transcription may involve local changes in chromatin activity in Drosophila. *Mech. Dev.* **52**, 343-355.

Festenstein, R., Pagakis, S. N., Hiragami, K., Lyon, D., Verreault, A., Sekkali, B. and Kioussis, D. (2003). Modulation of heterochromatin protein 1 dynamics in primary mammalian cells. *Science* **229**, 719-721.

Fischle, W., Wang, Y., Jacobs, S. A., Kim, Y., Allis, C. D. and Khorasanizadeh, S. (2003). Molecular basis for the discrimination of repressive methyl-lysine marks in histone H3 by Polycomb and HP1 chromodomains. *Genes Dev.* **17**, 1870-1881.

Fitzgerald, D. P. and Bender, W. (2001). Polycomb group repression reduces DNA accessibility. *Mol. Cell. Biol.* **21**, 6585-6597.

Francis, N. J. and Kingston, R. E. (2001). Mechanisms of transcriptional memory. *Nat. Rev. Mol. Cell Biol.* **2**, 409-421.

Francis, N. J., Kingston, R. E. and Woodcock, C. (2004). Chromatin compaction by a Polycomb Group protein complex. *Science* **306**, 1574-1577.

Franke, A., DeCamillis, M., Zink, D., Cheng, N., Brock, H. W. and Paro, R. (1992). Polycomb and polyhomeotic are constituents of a multimeric protein complex in chromatin of *Drosophila melanogaster*. *EMBO J.* **11**, 2941-2950.

Garcia-Bellido, A., PRipoll, P. and Morata, G. (1976). Developmental compartmentalization in the dorsal mesothoracic disc of Drosophila. *Dev. Biol.* **48**, 132-147.

Gaul, U. and Jäckle, H. (1989). Analysis of maternal effect mutant combinations elucidates regulation and function of the overlap of hunchback and Krüppel gene expression in the *Drosophila* blastoderm embryo. *Development* **107**, 651-662.

Grewal, S. I. and Moazed, D. (2003). Heterochromatin and epigenetic control of gene expression. *Science* **301**, 798-802.

Hernández, G., Lalioti, V., Vandekerckhove, J., Sierra, J. M. and Santarén, J. F. (2004). Identification and characterization of the expression of the translation initiation factor 4A (eIF4A) from Drosophila melanogaster. *Proteomics* **4**, 316-326.

Houtsmuller, A. B. and Vermeulen, W. (2001). Macromolecular dynamics in living cell nuclei revealed by fluorescence redistribution after photobleaching. *Histochem. Cell Biol.* **115**, 13-21.

Houtsmuller, A. B., Rademakers, S., Nigg, A. L., Hoogstraten, D., Hoeijmakers, J. H. J. and Vermeulen, W. (1999). Action of DNA repair endonuclease ERCC1/XPF in living cells. *Science* **284**, 958-961.

Kuzmichev, A., Nishioka, K., Erdjument-Bromage, H., Tempst, P. and Reinberg, D. (2002). Histone methyltransferase activity associated with a human multiprotein complex containing the Enhancer of Zeste protein. *Genes Dev.* **16**, 2893-2905.

Levine, S. S., Weiss, A., Erdjument-Bromage, H., Shao, Z., Tempst, P. and Kingston, R. E. (2002). The core of the polycomb repressive complex is compositionally and functionally conserved in flies and humans. *Mol. Cell. Biol.* **22**, 6070-6078.

Levine, S. S., King, I. F. G. and Kingston, R. E. (2004). Division of labor in Polycomb group repression. *Trends Biochem. Sci.* **29**, 478-485.

Lewis, E. B. (1963). Genes and developmental pathways. *Am. Zool.* **3**, 33-56.

Lewis, E. B. (1978). A gene complex controlling segmentation in Drosophila. *Nature* **276**, 565-570.

McNally, J. G., Müller, W. G., Walker, D., Wolford, R. and Hager, G. L. (2000). The glucocorticoid receptor: rapid exchange with regulatory sites in living cells. *Science* **287**, 1262-1265.

Milan, M., Diaz-Benjumea, F. L. and Cohen, S. M. (1998). Beadex encodes an LMO protein that regulates Apterous LIM-homeodomain activity in Drosophila wing development: a model for LMO oncogene function. *Genes Dev.* **12**, 2912-2920.

Min, J., Zhang, Y. and Xu, R. M. (2003). Structural basis for specific binding of Polycomb chromodomain to histone H3 methylated at Lys 27. *Genes Dev.* **17**, 1823-1828.

Misteli, T., Gunjan, A., Hock, R., Bustin, M. and Brown, D. T. (2000). Dynamic binding of histone H1 to chromatin in living cells. *Nature* **408**, 877-881.

Mulholland, N. M., King, I. F. G. and Kingston, R. E. (2003). Regulation of Polycomb roup complexes by the sequence-specific DNA binding proteins Zeste and GAGA. *Genes Dev.* **17**, 2741-2746.

Müller, J., Hart, C. M., Francis, N. J., Vargas, M. L., Sengupta, A., Wild, B., Miller, E. L., O'Connor, M. B., Kingston, R. E. and Simon, J. A. (2002). Histone methyltransferase activity of a Drosophila Polycomb group repressor complex. *Cell* **111**, 197-208.

Netter, S., Faucheux, M. and Theodore, L. (2001). Developmental dynamics of a polyhomeotic-EGFP fusion in vivo. *DNA Cell Biol.* **20**, 483-492.

Ng, J., Hart, C. M., Morgan, K. and Simon, J. A. (2000). A *Drosophila* ESC-E(Z) protein complex is distinct from other polycomb group complexes and contains covalently modified ESC. *Mol. Cell. Biol.* **20**, 3069-3078.

Orlando, V. (2003). Polycomb, epigenomes, and control of cell identity. *Cell* **112**, 599-606.

Orlando, V., Jane, E. P., Chinwalla, V., Harte, P. J. and Paro, R. (1998). Binding of trithorax and Polycomb proteins to the bithorax complex: dynamic changes during early *Drosophila* embryogenesis. *EMBO J.* **17**, 5141-5150.

Paro, R. and Hogness, D. S. (1991). The Polycomb protein shares a homologous domain with a heterochromatin-associated protein of Drosophila. *Proc. Natl. Acad. Sci. USA* **88**, 263-267.

Phair, R. D. and Misteli, T. (2001). Kinetic modeling approaches to in vivo imaging. *Nat. Rev. Mol. Cell Biol.* **2**, 898-907.

Phair, R. D., Scaffidi, P., Elbi, C., Vacerova, J., Dey, A., Ozato, K., Brown, D. T., Hager, G., Bustin, M. and Misteli, T. (2004). Global nature of dynamic protein-chromatin interactions in vivo: three dimensional genome scanning and dynamic interaction networks of chromatin proteins. *Mol. Cell. Biol.* **24**, 6393-6402.

Post, J. N., Lidke, K. A., Rieger, B. and Arndt-Jovin, D. J. (2005). One- and two-photon photoactivation of a paGFP-fusion protein in live Drosophila embryos. *FEBS Lett.* **579**, 325-330.

Rastelli, L., Chan, C. S. and Pirrotta, V. (1993). Related chromosome binding sites for *zeste*, suppressors of *zeste* and Polycomb group proteins in *Drosophila* and their dependence on *Enhancer of zeste* function. *EMBO J.* **12**, 1513-1522.

Ringrose, L., Rehmsmeier, M., Dura, J. M. and Paro, R. (2003). Genome-wide prediction of Polycomb/Trithorax response elements in Drosophila melanogaster. *Dev. Cell* **5**, 759-771.

Ringrose, L., Ehret, H. and Paro, R. (2004). Distinct contributions of histone H3 Lysine 9 and 27 Methylation to locus-specific stability of polycomb complexes. *Mol. Cell* **16**, 641.

Roy, G., Miron, M., Khaleghpour, K., Lasko, P. and Sonenberg, N. (2004). The Drosophila Poly(A) binding protein-interacting protein, dPaip2, is a novel effector of cell growth. *Mol. Cell. Biol.* **24**, 1143-1154.

Saurin, A. J., Shao, Z., Erdjument-Bromage, H., Tempst, P. and Kingston, R. E. (2001). A Drosophila Polycomb group complex includes ZESTE and dTAFII proteins. *Nature* **412**, 655-660.

Sengel, P. and Mandaron, P. (1969). Aspects morphologiques du développement in vitro des disques imaginaux de la Drosophila. *Arch. Dev. Biol.* **174**, 303-311.

Shao, Z. H., Raible, F., Mollaaghababa, R., Guyon, J. R., Wu, C. T., Bender, W. and Kingston, R. E. (1999). Stabilization of chromatin structure by PRC1, a Polycomb complex. *Cell* **98**, 37-46.

Simon, J. A. and Tamkun, J. W. (2002). Programming off and on states in chromatin: mechanism of Polycomb and trithorax group complexes. *Curr. Opin. Genet. Dev.* **12**, 210-218.

Spradling, A. C. and Rubin, G. M. (1982). Transposition of cloned P elements into Drosophila germ line chromosomes. *Science* **218**, 341-347.

Sprague, B. L., Pego, R. L., Stavreva, D. A. and McNally, J. G. (2004). Analysis of binding reactions by fluorescence recovery after photobleaching. *Biophys. J.* **86**, 3473-3495.

Strutt, H. and Paro, R. (1997). The Polycomb group protein complex of *Drosophila melanogaster* has different compositions at different target genes. *Mol. Cell. Biol.* **17**, 6773-6783.

Strutt, H., Cavalli, G. and Paro, R. (1997). Co-localization of Polycomb protein and GAGA factor on regulatory elements responsible for the maintenance of homeotic gene expression. *EMBO J.* **16**, 3621-3632.

Tautz, D. (1988). Regulation of the *Drosophila* segmentation gene hunchback by two maternal morphogenetic centres. *Nature* **332**, 281-284.

Verkman, A. S. (2002). Solute and macromolecule diffusion in cellular aqueous compartments. *Trends Biochem. Sci.* **27**, 27-33.

Vermaak, D., Ahmad, K. and Henikoff, S. (2003). Maintenance of chromatin states:an open-and-shut case. *Curr. Opin. Cell Biol.* **15**, 266-274.

Wang, L., Brown, J. L., Cao, R., Zhang, Y., Kassis, J. A. and Jones, R. S.

(2004). Hierarchical recruitment of Polycomb group silencing complexes. *Mol. Cell* **14**, 637-646.

White, J. and Stelzer, E. (1999). Photobleaching GFP reveals protein dynamics inside live cells. *Trends Cell Biol.* **9**, 61-65.

Yamamoto, K., Sonoda, M., Inokuchi, J., Shirasawa, S. and Sasazuki, T. (2004). Polycomb group suppressor of zeste 12 links heterochromatin protein 1α and enhancer of zeste 2. *J. Biol. Chem.* **279**, 401-406.